Mammalian Fbh1 is important to restore normal mitotic progression following decatenation stress

Corentin Laulier[1], **Anita Cheng**[1], **Nick Huang**[1], and **Jeremy M. Stark**[1,2]

[1]Department of Cancer Biology, Division of Radiation Biology, Beckman Research Institute of the City of Hope, 1500 E Duarte Rd., Duarte, CA 91010

Abstract

We have addressed the role of the F-box helicase 1 (Fbh1) protein during genome maintenance in mammalian cells. For this, we generated two mouse embryonic stem cell lines deficient for Fbh1: one with a homozygous deletion of the N-terminal F-box domain (*Fbh1$^{f/f}$*), and the other with a homozygous disruption (*Fbh1$^{-/-}$*). Consistent with previous reports of Fbh1-deficiency in vertebrate cells, we found that *Fbh1$^{-/-}$* cells show a moderate increase in Rad51 localization to DNA damage, but no clear defect in chromosome break repair. In contrast, we found that *Fbh1$^{f/f}$* cells show a decrease in Rad51 localization to DNA damage and increased cytoplasmic localization of Rad51. However, these *Fbh1$^{f/f}$* cells show no clear defects in chromosome break repair. Since some Rad51 partners and F-box-associated proteins (Skp1-Cul1) have been implicated in progression through mitosis, we considered whether Fbh1 might play a role in this process. To test this hypothesis, we disrupted mitosis using catalytic topoisomerase II inhibitors (bisdioxopiperazines), which inhibit chromosome decatenation. We found that both *Fbh1$^{f/f}$* and *Fbh1$^{-/-}$* cells show hypersensitivity to topoisomerase II catalytic inhibitors, even though the degree of decatenation stress was not affected. Furthermore, following topoisomerase II catalytic inhibition, both Fbh1-deficient cell lines show substantial defects in anaphase separation of chromosomes. These results indicate that Fbh1 is important for restoration of normal mitotic progression following decatenation stress.

Keywords

1. Introduction

Ubiquitin E3 ligase complexes promote the degradation of target proteins by the 26S proteasome, which is important for the regulation of protein stability during multiple cellular processes. SCF (Skp1-Cul1-F-box protein) complexes are part of the E3 complex family, where the F-box proteins function to recruit specific targets for ubiquitination [1,2]. Among the approximately 70 F-box proteins in mammalian cells, one protein contains a known catalytic

[2]Correspondence should be addressed to J.M.S: Phone: 626-359-8111 ext 63346, Fax: 626-301-8892, jstark@coh.org.

Conflict of interests
The authors declare that there are no conflicts of interest.

domain: Fbh1, for F-box helicase 1 [2]. Namely, in addition to an N-terminal F-box domain, Fbh1 also contains a C-terminal superfamily I 3' to 5' helicase domain [3,4].

In yeast, Fbh1 appears to be important for DNA repair by regulating the strandexchange protein Rad51. In *S. pombe*, Fbh1 forms nuclear foci after DNA damage and limits recombination at blocked replication forks by directly modulating Rad51 loading onto DNA [5–7]. In *S. cerevisiae*, expression of human Fbh1 suppresses recombination defects in *srs2*, which is a regulator of Rad51 [8]. However, a ubiquitination target for Fbh1 in *S. pombe*, ATF1, has no known role during DNA repair, suggesting that Fbh1 could be involved in additional cellular processes [9].

In vertebrates, studies of chicken DT40 lymphocytes showed that Fbh1 disruption does not affect either cellular sensitivity to DNA damaging agents or homology-directed repair (HDR) of a chromosomal double-strand break (DSB), but causes a slight increase in the frequency of sister chromatid exchanges (SCEs) [10]. In human U2OS cells, Fbh1-GFP fusion proteins co-localize with the single-stranded DNA binding protein RPA after ionizing radiation [11]. Also in U2OS cells, elevated levels of Fbh1 were shown to cause a decrease in both RAD51 ionizing-radiation-induced foci and HDR, and RNAi disruption of Fbh1 led to a modest increase in spontaneous RAD51 foci and SCEs [11].

Rad51 partners and SCF components have also been implicated in mitotic progression. Cells defective for BRCA2 or BARD1 show abnormal cytokinesis [12,13], and BRCA1 participates in DNA decatenation [14]. In addition, the Blm helicase promotes correct chromosome segregation by resolving entangled DNA structures during anaphase [15]. Furthermore, Skp1 and Cul1 associate with centrosomes that form the mitotic spindle [16], and Cul1 appears important for proper centrosome duplication during mitosis [17].

Recovery from a mitotic stress is an important aspect of normal mitotic progression [18]. In this study, we evaluated the response to a mitotic stress caused by inhibition of topoisomerase II, which we refer to as a decatenation stress. Namely, catalytic inhibition of topoisomerase II disrupts chromosome decatenation: a process that is important for chromosome condensation and sister chromatid separation [19,20]. Bisdioxopiperazines are common catalytic inhibitors of topoisomerase II used to protect cardiac tissue from the effects of clastogenic topoisomerase II poisons during cancer chemotherapy [21,22]. In contrast to these poisons, bisdioxopiperazines (e.g. ICRF-193 and razoxane) do not induce substantial levels of DSBs [23,24]. Rather, these compounds are specific inhibitors of the ATPase function of topoisomerase II, which causes a disruption in decatenation [22]. Given that stem cells do not contain a decatenation checkpoint, such cells progress through mitosis without resolving DNA topological problems induced by treatment with bisdioxopiperazines [25–27]. Because stem cells are proposed to play a role in cancer development [28], it is important to characterize the pathways that affect normal mitotic progression of stem cells after decatenation stress [19].

We sought to address the role of Fbh1 in chromosome break repair and mitotic progression in mouse embryonic stem (ES) cells. For this, we established two Fbh1-deficient ES cell lines: one containing a homozygous deletion of both the F-box and helicase domains (*Fbh1$^{−/−}$*), and another carrying a homozygous deletion of the F-box domain (*Fbh1$^{f/f}$*). With these cell lines, we found that Fbh1-deficient cells show moderate changes in Rad51 localization, but show no defect in chromosome break repair. Importantly, following topoisomerase II catalytic inhibition, we found that Fbh1-deficient cells show significant defects in clonogenic survival, anaphase separation of chromosomes, and nuclear structure. We suggest that Fbh1 is important for restoration of normal mitotic progression following decatenation stress.

2. Material and Methods

2.1. Plasmids and cell lines

Targeting vectors were generated using pF2L2neoDTa [29] by PCR of mouse genomic DNA: upstream arm 5'tgtaggaacacgggaacaca and 5'agatgctgcacactggacac, *Fbh1^f* downstream arm 5'tacagcttttggatcttgctca and 5'gaggttcctcaacagaatggacm, *Fbh1$^−$* downstream arm 5'gtcctcttcctccgtatgcttac and 5'gagacagatggctcttccgtact. SacII-linearized targeting vectors were electroporated in J1 mouse ES cells (ATCC) at 730V 10uF. Integrants were selected in G418 and targeting was assayed by PCR: p1 5'taagaccagcctcagctacttg, p2 5'taaaggtatgaaccaccacagc, p3 5'ggttccggatccactagttct, p4 5'tgcaaagaagaggcatacca, p5 5'agtgcatccagtcacactgc. The *neo* cassette was removed with electroporation of pCAGGS-CRE [30], prior to targeting the second allele. RT-PCR was performed using random primed reverse transcription of total RNA (Qiagen): e2 gcccttcagtcagagatgga, e5 gtcaacacttggggagcatt, e17 ttcgcttccagttccttgtc.

Expression vectors for Fbh1 (pCAG-Fbh1-3xFlag) and Fbh1f (pCAG-FBH1f-3xFlag) were generated in pCAGGS-BSKX [31] using the above RT-PCR products and MGC37007 (ATCC). The DR-GFP reporter was integrated by targeting to the pim1 locus, as previously described [32].

2.2. Sensitivity and HDR assays

Cells were seeded in a 12 well plate at different concentrations ranging from 1.5 to 9×10^4 cells per well. 24 h later, cells were treated with camptothecin (CPT, CAS: 7689-03-4), etoposide (CAS: 33419-42-0), ICRF-193 (CAS: 21416-88-6), razoxane (CAS: 21416-67-1) or with vehicle (DMSO). After 20 hours, cells were washed with PBS and recovered in fresh media for 5 days for all compounds except razoxane (4 days). For quantification of clonogenic survival, cells were fixed in 10% methanol, 10% acetic acid, stained with 1% crystal violet. Stained cells were dissolved with 0.1% SDS in methanol for quantification using a microplate reader at 570 nm [33]. Each clonogenic survival value represents the mean of at least three independent treatments. Cell survival was calculated relative to the mean value of the vehicle-treated cells for each experiment. HDR was measured as described previously [31].

2.3. Immunoblot

Transfections were performed using Lipofectamine 2000 (Invitrogen) with empty vector, pCAG-Fbh1-3xFlag, or pCAG-FBH1f-3xFlag. After two days, proteins were isolated by repeated freeze/thawing in NETN buffer (20mM Tris pH8, 100mM NaCl, 1mM EDTA, 0.5% IGEPAL, 1mM DTT) with Protease inhibitor cocktail (Roche). Equal amounts of total protein (8 µg) from each sample was separated on 4–12% SDS-PAGE, and probed with HRP conjugated anti-Flag M2 antibody (Sigma).

2.4. Immunofluorescence staining and time-lapse microscopy

To quantify Rad51 foci, cells were treated for 2 hours with CPT, then fixed in 2% paraformaldehyde for immunostaining with anti-Rad51 antibody (EMD4Biosciences PC130) and Alexa fluor 568 goat anti-rabbit IgG (Invitrogen). Images were acquired using an AX-70 microscope (Olympus). For real-time analysis of chromosome segregation, cells were stably transfected with pEGFP-N1-H2B [34]. Time-lapse microscopy was performed using a Zeiss Observer inverted microscope on untreated cells, and cells treated with ICRF-193 (100nM) for 20 hours, followed by 20 hours of recovery. Images were collected using Image-Pro software (Media Cybernetics) and a 40x NA 0.75 UPlanFl objective.

2.5. Metaphase chromosomes and nuclear morphology analysis

For mitotic chromosome analysis, after a 2-hour treatment with colcemid (1µg/ml) (Gibco), cells were incubated in hypotonic solution (0.075 M KCl) for 6 min at 37 °C, followed by 2 rounds of wash in fixative solution (3:1 methanol/glacial acetic acid). Cells were then spread on slides and chromosomes were stained with 4% Giemsa (Gibco). To quantify aberrant nuclei, we used the same hypotonic solution and fixative solution treatment as described above, before nuclei were spread on slides. 800 to 1300 nuclei were analyzed in 5 independent experiments.

2.6. Statistical analysis

Error bars represent the standard deviation from the mean. Statistical analysis was performed using the unpaired t-test for Rad51 foci, HDR, clonogenic survival, metaphase duration, and nuclear abnormality experiments. The two-tailed Fisher's exact test was used for statistical analysis of the anaphase separation experiments.

3. Results

3.1. Generation of two homozygous Fbh1-deficient mouse ES cell lines

We sought to address the role of Fbh1 in mammalian cells by generating mouse ES cell lines with homozygous mutations for two distinct alleles of *Fbh1*. The first allele, *Fbh1⁻*, is a deletion of exons 3–12 including both the F-box and helicase domains (Fig. 1A). The other allele, *Fbh1ᶠ*, contains a deletion of exon 3, which encodes the F-box domain. In the absence of exon 3, the splicing of exons 2 and 4 would generate an mRNA that contains an alternative translation start codon positioned in exon 2, which could encode an N-terminal deleted Fbh1 protein (Fbh1^f, Fig. 1A). Using targeting vectors for these deletion alleles, we generated homozygous mutant cell lines for both the *Fbh1ᶠ* and *Fbh1⁻* alleles in WT mouse ES cells, by performing two rounds of targeting (Fig. 1A, B). Subsequently, we confirmed expression of the predicted mRNA product in the resultant *Fbh1ᶠ/ᶠ* and *Fbh1⁻/⁻* cell lines using RT-PCR and sequencing of the amplification products (Fig. 1C, data not shown). Unfortunately, using three distinct antibodies directed against Fbh1, we were unable to detect Fbh1 signal in WT cells by either immunoblotting or indirect immunofluorescence (data not shown).

To test the potential coding capacity of the *Fbh1ᶠ* allele, we constructed Fbh1 expression plasmids carrying the wild-type (*Fbh1⁺*) and *Fbh1ᶠ* cDNAs, with a 3xFlag-tag sequence at the 3' end. After transient transfection of mouse ES cells, Fbh1 expression was measured by immunoblotting using an anti-Flag antibody (Fig. 1D). Both *Fbh1⁺* and *Fbh1ᶠ* were efficiently expressed, confirming that the alternative translation start in exon 2 of *Fbh1ᶠ* is functional. Moreover, the expression level of the Fbh1^f protein appears higher than for Fbh1$^+$ (5-fold, Fig. 1D). This finding is consistent with analysis of human Fbh1 expressed in *S. cerevisiae*, which showed an increased stability of an F-box-deficient protein compared to FBH1$^+$ [8]. These results indicate that the *Fbh1ᶠ* allele can express an N-terminal truncated protein that lacks the F-box but retains the conserved helicase domain.

3.2. Fbh1 affects Rad51 localization, but has no apparent role during chromosome break repair

We considered that Fbh1-deficiency in mouse ES cells could affect Rad51 localization and/or chromosome break repair. Recently, in U2OS cells, RNAi-mediated depletion of Fbh1 caused a modest increase in spontaneous Rad51 foci, and elevated levels of WT Fbh1 showed diminished Rad51 foci following DNA damage [11]. As well, Fbh1-deficient *S. pombe* were shown to exhibit elevated levels of spontaneous Rad51 foci [5]. Thus, we analyzed the ability of *Fbh1ᶠ/ᶠ* and *Fbh1⁻/⁻* ES cells to form Rad51 foci after treatment with CPT. Cells were incubated for 2 hours with 50nM CPT and Rad51 foci formation was measured by

immunofluorescence (Fig. 2A). This CPT treatment caused a significant induction of Rad51 foci in wild-type (WT) cells (31% of cells), and an even greater induction in $Fbh1^{-/-}$ cells (48% of cells). Thus, loss of Fbh1 causes a modest increase in Rad51 foci formation compared to WT cells (1.5-fold, p=0.014). In contrast to this elevation in $Fbh1^{-/-}$ cells, $Fbh1^{f/f}$ cells showed reduced levels of Rad51 foci (11% of cells, 2.8-fold reduction relative to WT, p=0.0003). Furthermore, we observed an increase in cytoplasmic staining of Rad51 in $Fbh1^{f/f}$ cells (Fig. 2B), compared to WT (6-fold, p<0.001). Thus, endogenous expression of an Fbh1 protein that lacks the F-box domain, but retains the conserved helicase domain, reduces Rad51 recruitment to CPT-induced damage. These results indicate that F-box-mediated functions of Fbh1 are important for efficient localization of Rad51 to DNA damage. Such F-box mediated functions could include regulation of Fbh1 expression levels and/or helicase activity, among other possible mechanisms.

Because Rad51 is a key factor in homologous recombination [35], we then addressed whether Fbh1-deficiency might affect HDR of DSBs, using the DR-GFP reporter [32]. Repair of an I-SceI endonuclease-generated DSB in DR-GFP by the HDR pathway results in restoration of a functional *GFP* cassette. This method was used in a recent report to show that elevated levels of Fbh1 cause a decrease in HDR in human U2OS cells [11], and a similar method was used to show that $Fbh1^{-/-}$ chicken DT40 cells exhibit no change in HDR compared to WT [10]. To test the effect of Fbh1-disruption and F-box-deletion on HDR in mammalian cells, we integrated DR-GFP at the *pim1* locus of the $Fbh1^{-/-}$, $Fbh1^{f/f}$, and WT cell lines. With these cell lines, we measured the frequency of GFP+ cells following transient expression of I-SceI. From these experiments, we found no difference between the $Fbh1^{-/-}$, $Fbh1^{f/f}$, and WT cell lines in the efficiency of HDR (Fig. 2C).

To further address chromosome break repair in Fbh1-deficient ES cells, we determined their sensitivity to clastogenic agents. Specifically, we treated cells for 20 hours with varying concentrations of either CPT or etoposide, which poisons topoisomerase II, causing DSBs. We then measured clonogenic survival after 5 days of recovery. From these experiments, we found that the sensitivity of $Fbh1^{f/f}$ and $Fbh1^{-/-}$ cells to both CPT and etoposide was indistinguishable from WT cells (Figs. 2D and 2E, respectively). Thus, Fbh1-deficiency does not affect cellular sensitivity to chromosome breaks formed by topoisomerase poisons. These data suggest that while Fbh1 modestly affects Rad51 localization to CPT-induced damage, neither Fbh1-disruption nor F-box-deletion appear to significantly affect chromosome break repair in mammalian cells. These results are consistent with previous findings that WT and $Fbh1^{-/-}$ chicken DT40 cells show similar sensitivity to a number of DNA damaging agents [10].

3.3. Fbh1 is important for survival following decatenation stress

We next searched for another role for Fbh1 during chromosome maintenance. As several Rad51 partners, as well as SCF components, have been implicated in multiple aspects of mitosis [12–15,36], we considered that Fbh1 might affect mitotic progression. To address this hypothesis, we characterized the consequences of a mitotic stress induced by two bisdioxopiperazines (ICRF-193 and razoxane), which inhibit topoisomerase II catalytic activity, resulting in the disruption of chromosome decatenation [22,27].

First, we determined the effect of ICRF-193 and razoxane on clonogenic survival of WT, $Fbh1^{f/f}$, and $Fbh1^{-/-}$ cell lines. Cells were exposed to ICRF-193 or razoxane for 20 hours, followed by several days of recovery before determining clonogenic survival (4 days for razoxane, 5 days for ICRF-193). From these experiments, we found that both $Fbh1^{-/-}$ and $Fbh1^{f/f}$ cells showed significant hypersensitivity to ICRF-193 as compared to WT (Fig. 3A left panel, survival reduced 2-fold and 5-fold respectively following 200nM ICRF-193, p=0.0002). Similarly, we found that $Fbh1^{-/-}$ and $Fbh1^{f/f}$ cells showed hypersensitivity to razoxane as

compared to WT (Fig. 3A right panel, survival for both reduced 5-fold following treatment with 10μM razoxane, p=0.03). These results indicate that Fbh1 is important for survival after a decatenation stress induced by two different catalytic inhibitors of topoisomerase II.

3.4. ICRF-193 treatment causes a similar decatenation stress in WT and Fbh1-deficient cells

We next sought to examine the cause of the above hypersensitivity to topoisomerase II inhibition. For the below analyses, we used ICRF-193, which is the most potent topoisomerase II inhibitor among bisdioxopiperazines compounds [37,38], and affects clonogenic survival at a much lower dose than razoxane (see Figure 3A, Section 3.3).

First, we determined the effect of Fbh1-deficiency on chromosome condensation during mitosis, which requires topoisomerase II activity [39]. ES cells were left untreated or were treated for 2 hours with ICRF-193. We then analyzed the degree of chromosome condensation on metaphase spreads, as determined by the relative compaction of chromosomes. Without treatment, we found normal chromosome compaction in all of the cell lines (Fig. 3B). After ICRF-193 treatment, we observed the appearance of undercondensed chromosomal segments at the centromeric extremity (mouse chromosomes are telocentric, Fig. 3B). Regarding frequency, at least 70% of metaphase spreads from each cell line showed evidence of undercondensed chromosomes after ICRF-193 treatment (Fig. 3B). Furthermore, we found no statistical difference between WT and Fbh1-deficient cells in the frequency of these events. Thus, Fbh1-deficiency does not appear to affect the degree of chromosome undercondensation caused by ICRF-193 treatment.

For a second measure of the degree of decatenation stress, we analyzed the localization of PICH (Plk1-Interacting Checkpoint Helicase) during metaphase. PICH is a member of the SWI/SNF2 family of DNA-dependent ATPases [40]. Interestingly, PICH associates in threads at chromosomal regions that undergo a late decatenation during mitosis [41,42]. Using this method, we observed an equivalent induction of metaphases with PICH threads after treatment with ICRF-193 in WT, *Fbh1$^{f/f}$* and *Fbh1$^{-/-}$* cells (Fig. 3C). These results indicate that ICRF-193 treatment causes a similar decatenation stress in WT, *Fbh1$^{f/f}$*, and *Fbh1$^{-/-}$* cells.

3.5. Fbh1-deficient cells fail to restore a normal mitosis after decatenation stress

Since ICRF-193 treatment causes disruption of mitotic chromosome condensation and separation at anaphase [25,43], survival following this decatenation stress likely requires restoration of normal mitotic progression in subsequent divisions, particularly since ES cells lack a decatenation checkpoint [26]. Thus, we hypothesized that Fbh1 might be important for this recovery process. To address this, we established WT, *Fbh1$^{f/f}$*, and *Fbh1$^{-/-}$* cell lines that stably express the GFP-tagged histone H2B. GFP-H2B expression enables real-time visualization of chromosome dynamics [34]. With these cell lines, we acquired images every 2 minutes for 3 hours, and each cell showing evidence of chromosome condensation was then scored for clear separation of chromosomes at anaphase (Fig. 4A left panels, Movie S1). Mitotic cells that failed to resolve into two distinct daughter nuclei were scored as showing abnormal anaphase separation (Fig. 4A right panels, Movie S2).

To begin with, we analyzed mitotic progression of individual cells without any stress. For each of the cell lines, the vast majority of cells showed clear anaphase separation into two daughter cells (95% for WT, 91% for *Fbh1$^{f/f}$*, and 86% for *Fbh1$^{-/-}$*, Fig. 4B and Table 1). The *Fbh1$^{-/-}$* cells showed a slightly lower percentage of normal anaphase progression compared to WT, but this difference was not statistically significant since abnormal anaphase separation is an uncommon event in all the cell lines.

We next determined the ability of cells to restore normal mitotic progression following a decatenation stress. Cells were treated with 100nM ICRF-193 for 20 hours, followed by another 20 hours for recovery. We used a low dose of ICRF-193, as we predicted that WT cells should mostly be able to recover from this decatenation stress (see Fig. 3A, Section 3.3), whereas a higher dose of ICRF-193 (e.g. >2 μM) would cause a complete defect in chromosome condensation [26,43]. Indeed, only 10.2% of WT cells showed abnormal anaphase separation following this decatenation stress, which was not statistically different from untreated cells (5.6%, Fig. 4B and Table 1). Thus, WT cells are proficient at recovering normal anaphase separation following the decatenation stress. In contrast, $Fbh1^{f/f}$ and $Fbh1^{-/-}$ cells treated with decatenation stress showed a striking percentage of mitotic cells with abnormal anaphase separation (33.9% and 30.7%, respectively, Fig. 4B and Table 1), which was statistically different both from the untreated cells (p=0.001, and p=0.009, respectively), as well as treated WT cells (p=0.004, and p=0.001, respectively). These results indicate that Fbh1 is important to restore normal anaphase separation after decatenation stress.

Many cells also showed a delay in the completion of metaphase following decatenation stress (Fig. 4A and 4B). We observed increased metaphase duration following decatenation stress in WT (p=0.0003), $Fbh1^{f/f}$ (p=0.003), and $Fbh1^{-/-}$ (p=0.006) cells, compared to untreated cells. Importantly, this increase in metaphase duration was more substantial in Fbh1-deficient cells, as compared to WT (p=0.01 for $Fbh1^{f/f}$, p=0.02 for $Fbh1^{-/-}$). Thus, by the measures of both anaphase separation and the duration of mitosis, Fbh1 appears important to restore normal mitotic progression after decatenation stress.

We next sought to determine the consequences of Fbh1 deficiency on the outcome of mitosis by quantifying nuclear aberrations. In particular, massive chromosome segregation defects can be assayed by the formation of multilobed nuclei [44]. So, we wanted to determine whether the defect in mitotic progression in Fbh1-deficienct cells is associated with the formation of multilobed nuclei. For this, cells were treated with the same decatenation stress and recovery period as for the time-lapse microscopy experiments. Again, we used a low dose of ICRF-193, as we predicted that WT cells would mostly be able to recover from this decatenation stress (see Fig. 3A, Section 3.3); whereas a high dose of ICRF-193 (e.g. >2 μM) would cause significant induction of multilobed nuclei even in WT cells [43]. Using these samples, we spread nuclei onto slides, and scored individual nuclei as normal or multilobed (Fig. 4C). In these experiments, the decatenation stress did not induce the formation of multilobed nuclei in WT cells (less than 1% of nuclei, Fig. 4D). In contrast, we observed a significant induction of multilobed nuclei in $Fbh1^{f/f}$ and $Fbh1^{-/-}$ cell lines (more than 5% of nuclei, Fbh1-deficient cells different from WT at p<0.0002, Fig. 4D). Thus, Fbh1 appears important to limit the formation of multilobed nuclei following decatenation stress.

During the above analysis of nuclear abnormality, we also quantified the formation of micronuclei, which are proposed to result from lagging chromosomes and anaphase bridges [45]. From this analysis, we found that all the cell lines showed an increase in micronuclei following decatenation stress, although the Fbh1-deficient cells showed a higher frequency than WT (12% for $Fbh1^{f/f}$, 13% for $Fbh1^{-/-}$, and 7% for WT, Fbh1-deficient cells different from WT at p<0.003, Fig. 4D). In summary, Fbh1-deficient cells exposed to a decatenation stress, relative to WT cells, show substantial increases in defective anaphase separation and multilobed nuclei, as well as moderate increases in metaphase duration and micronuclei. These findings indicate that Fbh1 in mammalian cells is important to restore normal mitotic progression following decatenation stress.

4. Discussion

Our study is the first description of *Fbh1* gene disruption in mammalian cells, and provides evidence for a novel role of Fbh1 during the restoration of normal mitotic progression after decatenation stress. Furthermore, we characterized the role of Fbh1 during Rad51 recruitment to CPT-induced DNA damage, as well as chromosome break repair. Consistent with previous reports in vertebrate cells, Fbh1-deficiency caused a mild increase in Rad51 recruitment to DNA damage [11]. In addition, we show that deletion of the F-box domain causes a defect in Rad51 nuclear localization and recruitment to DNA damage. Thus, given that the Fbh1^f protein is expressed at elevated levels compared to the WT protein, F-box-dependent suppression of Fbh1 expression levels and/or helicase activity might be important for efficient localization of Rad51 to DNA damage. Accordingly, it was previously shown that Fbh1 over-expression in U2OS and *S. Pombe* results in reduced localization of Rad51 to DNA damages [5,11]. Nevertheless, we find that neither the *Fbh1$^{-/-}$* nor the *Fbh1$^{f/f}$* cells show a clear defect in chromosome break repair, which is consistent with previous findings with *Fbh1$^{-/-}$* DT40 chicken lymphocytes [10]. We suggest that the modest alterations in Rad51 localization mediated by Fbh1 are not sufficient to substantially affect chromosome break repair in mammalian cells.

However, such changes in Rad51 localization could be linked to the mitotic progression defects of Fbh1-deficient cells. This model is supported by recent evidence that Rad51-regulation is important for mitosis, in that another Rad51 modulator, Brca2, is important for mitotic progression [46]. Regarding our findings with Fbh1, decatenation stress could generate replication intermediates that require Fbh1-mediated regulation of Rad51 for their resolution, which subsequently could be important for mitotic progression. Since both cell lines show hypersensitivity to ICRF-193, it is important to consider that either inhibition or over-activation of Rad51 could disrupt Rad51-mediated functions during decatenation stress.

Alternatively, Fbh1 could affect recovery from decatenation stress by other mechanisms. For instance, Fbh1 could function similarly to other factors important for clonogenic survival after decatenation stress, which include BLM and proteins implicated in NHEJ, such as Ku, Ligase 4 and Metnase [15,47,48]. As has been proposed for BLM [15], Fbh1 could be involved the resolution of anaphase chromatin bridges that appear during decatenation stress. Fbh1 could also play a similar role as the NHEJ factors, though this may be unlikely given that Fbh1-deficient cells showed no hypersensitivity to etoposide treatment, which is distinct from NHEJ-deficient cells [47]. More generally, Fbh1 could be important for the resolution of topological problems that accumulate after topoisomerase II inhibition, thereby suppressing formation of aberrant DNA structures that could affect chromosome segregation. Apart from any DNA replication/repair function, Fbh1 may act directly in the regulation of mitotic progression through F-box-dependent recruitment of target proteins for SCF-mediated ubiquitination. Consistent with this latter possibility, deletion of the Fbh1 F-box domain alone is sufficient to induce hypersensitivity to ICRF-193.

Decatenation stress can lead to abnormal chromosome segregation and aneuploidy [49], which has long been proposed to contribute to the etiology of cancer [50]. To limit the genotoxic consequences of decatenation stress, many mammalian cells activate the decatenation checkpoint to delay mitosis onset [24,51]. However, this decatenation checkpoint is defective in stem cells [26]. Thus, stem cells may rely on alternative pathways to ensure normal mitotic progression following decatenation stress. Here we have presented evidence that Fbh1 is an important factor for this process. As bisdioxopiperazines are used during cancer therapy [21], it will be important to further characterize the range of mechanisms that protect the genomic integrity of stem cells from decatenation stress.

Supplementary Material

Refer to Web version on PubMed Central for supplementary material.

Acknowledgments

References

1. Skowyra D, Craig KL, Tyers M, Elledge SJ, Harper JW. F-box proteins are receptors that recruit phosphorylated substrates to the SCF ubiquitin-ligase complex. Cell 1997;91:209–219. [PubMed: 9346238]

2. Jin J, Cardozo T, Lovering RC, Elledge SJ, Pagano M, Harper JW. Systematic analysis and nomenclature of mammalian F-box proteins. Genes Dev 2004;18:2573–2580. [PubMed: 15520277]

3. Kim J, Kim JH, Lee SH, Kim DH, Kang HY, Bae SH, Pan ZQ, Seo YS. The novel human DNA helicase hFBH1 is an F-box protein. J Biol Chem 2002;277:24530–24537. [PubMed: 11956208]

4. Kim JH, Kim J, Kim DH, Ryu GH, Bae SH, Seo YS. SCFhFBH1 can act as helicase and E3 ubiquitin ligase. Nucleic Acids Res 2004;32:2287–2297. [PubMed: 15118074]

5. Lorenz A, Osman F, Folkyte V, Sofueva S, Whitby MC. Fbh1 Limits Rad51-dependent Recombination at Blocked Replication Forks. Mol Cell Biol. 2009

6. Morishita T, Furukawa F, Sakaguchi C, Toda T, Carr AM, Iwasaki H, Shinagawa H. Role of the Schizosaccharomyces pombe F-Box DNA helicase in processing recombination intermediates. Mol Cell Biol 2005;25:8074–8083. [PubMed: 16135799]

7. Osman F, Dixon J, Barr AR, Whitby MC. The F-Box DNA helicase Fbh1 prevents Rhp51-dependent recombination without mediator proteins. Mol Cell Biol 2005;25:8084–8096. [PubMed: 16135800]

8. Chiolo I, Saponaro M, Baryshnikova A, Kim JH, Seo YS, Liberi G. The human F-Box DNA helicase FBH1 faces Saccharomyces cerevisiae Srs2 and postreplication repair pathway roles. Mol Cell Biol 2007;27:7439–7450. [PubMed: 17724085]

9. Lawrence CL, Jones N, Wilkinson CR. Stress-Induced Phosphorylation of S. pombe Atf1 Abrogates Its Interaction with F Box Protein Fbh1. Curr Biol 2009;19:1907–1911. [PubMed: 19836238]

10. Kohzaki M, Hatanaka A, Sonoda E, Yamazoe M, Kikuchi K, Vu Trung N, Szuts D, Sale JE, Shinagawa H, Watanabe M, Takeda S. Cooperative roles of vertebrate Fbh1 and Blm DNA helicases in avoidance of crossovers during recombination initiated by replication fork collapse. Mol Cell Biol 2007;27:2812–2820. [PubMed: 17283053]

11. Fugger K, Mistrik M, Danielsen JR, Dinant C, Falck J, Bartek J, Lukas J, Mailand N. Human Fbh1 helicase contributes to genome maintenance via pro- and anti-recombinase activities. J Cell Biol 2009;186:655–663. [PubMed: 19736316]

12. Daniels MJ, Wang Y, Lee M, Venkitaraman AR. Abnormal cytokinesis in cells deficient in the breast cancer susceptibility protein BRCA2. Science 2004;306:876–879. [PubMed: 15375219]

13. Ryser S, Dizin E, Jefford CE, Delaval B, Gagos S, Christodoulidou A, Krause KH, Birnbaum D, Irminger-Finger I. Distinct roles of BARD1 isoforms in mitosis: full-length BARD1 mediates Aurora B degradation, cancer-associated BARD1beta scaffolds Aurora B and BRCA2. Cancer Res 2009;69:1125–1134. [PubMed: 19176389]

14. Lou Z, Minter-Dykhouse K, Chen J. BRCA1 participates in DNA decatenation. Nat Struct Mol Biol 2005;12:589–593. [PubMed: 15965487]

15. Chan KL, North PS, Hickson ID. BLM is required for faithful chromosome segregation and its localization defines a class of ultrafine anaphase bridges. Embo J 2007;26:3397–3409. [PubMed: 17599064]

16. Freed E, Lacey KR, Huie P, Lyapina SA, Deshaies RJ, Stearns T, Jackson PK. Components of an SCF ubiquitin ligase localize to the centrosome and regulate the centrosome duplication cycle. Genes Dev 1999;13:2242–2257. [PubMed: 10485847]

17. Korzeniewski N, Zheng L, Cuevas R, Parry J, Chatterjee P, Anderton B, Duensing A, Munger K, Duensing S. Cullin 1 functions as a centrosomal suppressor of centriole multiplication by regulating polo-like kinase 4 protein levels. Cancer Res 2009;69:6668–6675. [PubMed: 19679553]

18. Kops GJ, Weaver BA, Cleveland DW. On the road to cancer: aneuploidy and the mitotic checkpoint. Nat Rev Cancer 2005;5:773–785. [PubMed: 16195750]

19. Damelin M, Bestor TH. The decatenation checkpoint. Br J Cancer 2007;96:201–205. [PubMed: 17211475]

20. Baxter J, Diffley JF. Topoisomerase II inactivation prevents the completion of DNA replication in budding yeast. Mol Cell 2008;30:790–802. [PubMed: 18570880]

21. Hensley ML, Hagerty KL, Kewalramani T, Green DM, Meropol NJ, Wasserman TH, Cohen GI, Emami B, Gradishar WJ, Mitchell RB, Thigpen JT, Trotti A III, von Hoff D, Schuchter LM. American Society of Clinical Oncology 2008 Clinical Practice Guideline Update: Use of Chemotherapy and Radiation Therapy Protectants. Journal of Clinical Oncology 2009;27:127–145. [PubMed: 19018081]

22. Nitiss JL. Targeting DNA topoisomerase II in cancer chemotherapy. Nat Rev Cancer 2009;9:338–350. [PubMed: 19377506]

23. Downes CS, Clarke DJ, Mullinger AM, Gimenez-Abian JF, Creighton AM, Johnson RT. A topoisomerase II-dependent G2 cycle checkpoint in mammalian cells. Nature 1994;372:467–470. [PubMed: 7984241]

24. Skoufias DA, Lacroix FB, Andreassen PR, Wilson L, Margolis RL. Inhibition of DNA decatenation but not DNA damage, arrests cells at metaphase. Mol Cell 2004;15:977–990. [PubMed: 15383286]

25. Clarke DJ, Johnson RT, Downes CS. Topoisomerase II inhibition prevents anaphase chromatid segregation in mammalian cells independently of the generation of DNA strand breaks. J Cell Sci 1993;105(Pt 2):563–569. [PubMed: 8408285]

26. Damelin M, Sun YE, Sodja VB, Bestor TH. Decatenation checkpoint deficiency in stem and progenitor cells. Cancer Cell 2005;8:479–484. [PubMed: 16338661]

27. Gorbsky GJ. Cell cycle progression and chromosome segregation in mammalian cells cultured in the presence of the topoisomerase II inhibitors ICRF-187 [(+)-1,2-bis(3,5-dioxopiperazinyl-1-yl) propane; ADR-529] and ICRF-159 (Razoxane). Cancer Res 1994;54:1042–1048. [PubMed: 8313360]

28. Reya T, Morrison SJ, Clarke MF, Weissman IL. Stem cells, cancer, and cancer stem cells. Nature 2001;414:105–111. [PubMed: 11689955]

29. Hoch RV, Soriano P. Context-specific requirements for Fgfr1 signaling through Frs2 and Frs3 during mouse development. Development 2006;133:663–673. [PubMed: 16421190]

30. Stark JM, Jasin M. Extensive loss of heterozygosity is suppressed during homologous repair of chromosomal breaks. Mol Cell Biol 2003;23:733–743. [PubMed: 12509470]

31. Bennardo N, Cheng A, Huang N, Stark JM. Alternative-NHEJ is a mechanistically distinct pathway of mammalian chromosome break repair. PLoS Genet 2008;4 e1000110.

32. Moynahan ME, Pierce AJ, Jasin M. BRCA2 is required for homology-directed repair of chromosomal breaks. Mol Cell 2001;7:263–272. [PubMed: 11239455]

33. Taniguchi T, Garcia-Higuera I, Xu B, Andreassen PR, Gregory RC, Kim ST, Lane WS, Kastan MB, D'Andrea AD. Convergence of the fanconi anemia and ataxia telangiectasia signaling pathways. Cell 2002;109:459–472. [PubMed: 12086603]

34. Kanda T, Sullivan KF, Wahl GM. Histone-GFP fusion protein enables sensitive analysis of chromosome dynamics in living mammalian cells. Curr Biol 1998;8:377–385. [PubMed: 9545195]

35. Sung P, Krejci L, Van Komen S, Sehorn MG. Rad51 recombinase and recombination mediators. J Biol Chem 2003;278:42729–42732. [PubMed: 12912992]

36. Cardozo T, Pagano M. The SCF ubiquitin ligase: insights into a molecular machine. Nat Rev Mol Cell Biol 2004;5:739–751. [PubMed: 15340381]

37. Hasinoff BB, Kuschak TI, Yalowich JC, Creighton AM. A QSAR study comparing the cytotoxicity and DNA topoisomerase II inhibitory effects of bisdioxopiperazine analogs of ICRF-187 (dexrazoxane). Biochem Pharmacol 1995;50:953–958. [PubMed: 7575679]

38. Tanabe K, Ikegami Y, Ishida R, Andoh T. Inhibition of topoisomerase II by antitumor agents bis(2,6-dioxopiperazine) derivatives. Cancer Res 1991;51:4903–4908. [PubMed: 1654204]

39. Nitiss JL. DNA topoisomerase II and its growing repertoire of biological functions. Nat Rev Cancer 2009;9:327–337. [PubMed: 19377505]

40. Chen XG, Li Y, Zang MX, Pei XR, Xu YJ, Gao LF. cDNA cloning and expression analysis of mouse gene encoding the protein Ercc6l which is a novel member of SNF2 family. Progress in Biochemistry and Biophysics 2004;31:443–448.

41. Baumann C, Korner R, Hofmann K, Nigg EA. PICH, a Centromere-Associated SNF2 Family ATPase, is regulated by Plk1 and required for the spindle checkpoint 2007;128:101–114.

42. Spence JM, Phua HH, Mills W, Carpenter AJ, Porter AC, Farr CJ. Depletion of topoisomerase IIalpha leads to shortening of the metaphase interkinetochore distance and abnormal persistence of PICH-coated anaphase threads. J Cell Sci 2007;120:3952–3964. [PubMed: 17956945]

43. Ishida R, Miki T, Narita T, Yui R, Sato M, Utsumi KR, Tanabe K, Andoh T. Inhibition of intracellular topoisomerase II by antitumor bis(2,6-dioxopiperazine) derivatives: mode of cell growth inhibition distinct from that of cleavable complex-forming type inhibitors. Cancer Res 1991;51:4909–4916. [PubMed: 1654205]

44. Fenech M. Cytokinesis-block micronucleus assay evolves into a "cytome" assay of chromosomal instability, mitotic dysfunction and cell death. Mutat Res 2006;600:58–66. [PubMed: 16822529]

45. Norppa H, Falck GC. What do human micronuclei contain? Mutagenesis 2003;18:221–233. [PubMed: 12714687]

46. Ayoub N, Rajendra E, Su X, Jeyasekharan AD, Mahen R, Venkitaraman AR. The Carboxyl Terminus of Brca2 Links the Disassembly of Rad51 Complexes to Mitotic Entry. Curr Biol. 2009

47. Adachi N, Suzuki H, Iiizumi S, Koyama H. Hypersensitivity of nonhomologous DNA end-joining mutants to VP-16 and ICRF-193: implications for the repair of topoisomerase II-mediated DNA damage. J Biol Chem 2003;278:35897–35902. [PubMed: 12842886]

48. Wray J, Williamson EA, Royce M, Shaheen M, Beck BD, Lee SH, Nickoloff JA, Hromas R. Metnase mediates resistance to topoisomerase II inhibitors in breast cancer cells. PLoS One 2009;4:e5323. [PubMed: 19390626]

49. Ishida R, Sato M, Narita T, Utsumi KR, Nishimoto T, Morita T, Nagata H, Andoh T. Inhibition of DNA topoisomerase II by ICRF-193 induces polyploidization by uncoupling chromosome dynamics from other cell cycle events. J Cell Biol 1994;126:1341–1351. [PubMed: 8089169]

50. Boveri T. Concerning the origin of malignant tumours by Theodor Boveri. Translated and annotated by Henry Harris. J Cell Sci 2008;121:1–84. [PubMed: 18089652]

51. Deming PB, Cistulli CA, Zhao H, Graves PR, Piwnica-Worms H, Paules RS, Downes CS, Kaufmann WK. The human decatenation checkpoint. Proc Natl Acad Sci U S A 2001;98:12044–12049. [PubMed: 11593014]
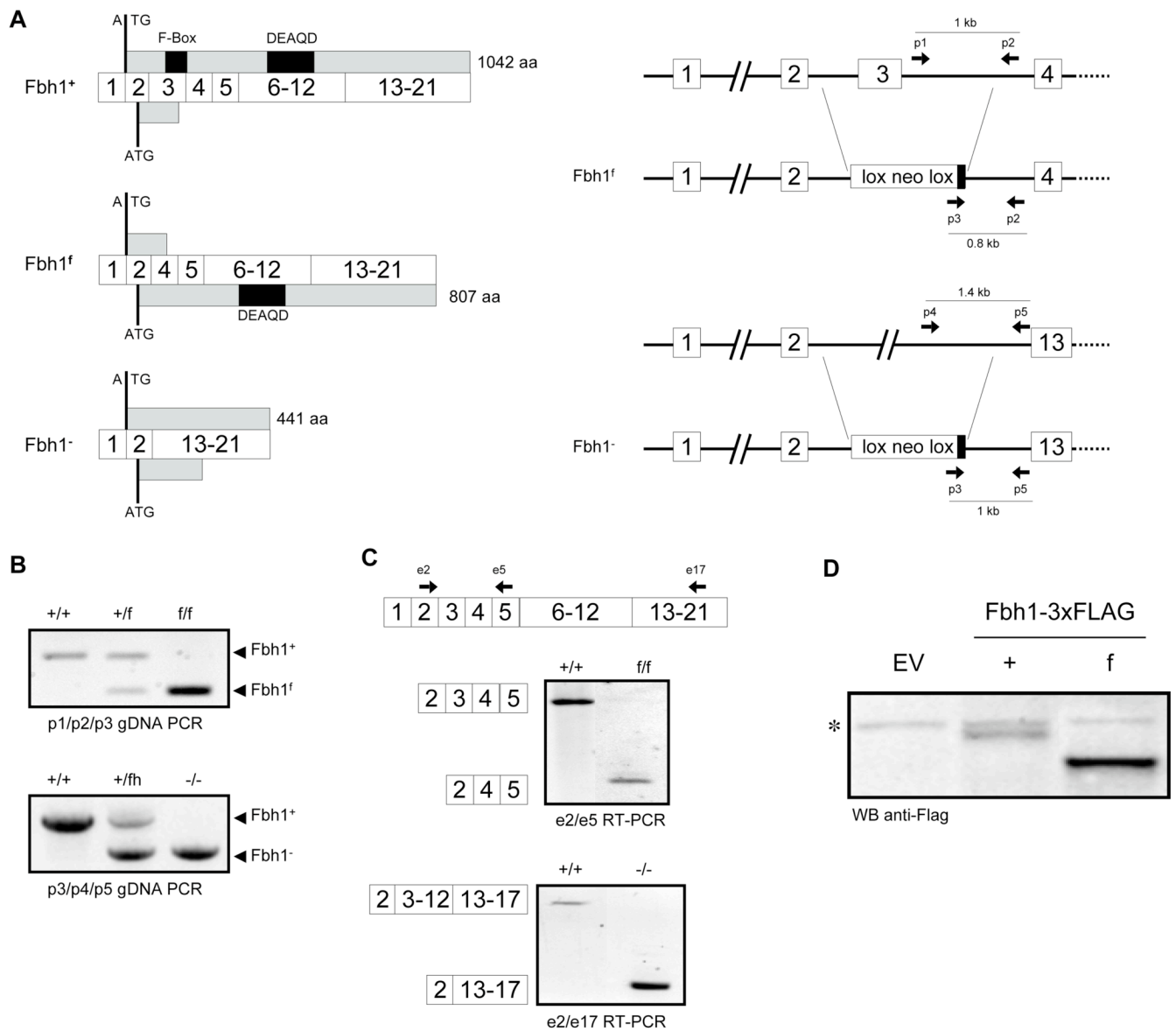
Fig. 1. Fbh1-deficient cell lines

A. Shown are diagrams of predicted transcripts (numbered boxes) and translation products (grey boxes) produced by different *Fbh1* alleles from two different start codons. The *Fbh1+* mRNA encodes a complete protein when the first start codon is used, the *Fbh1−* mRNA encodes a protein lacking both the F-box and helicase (DEAQD) domains, whereas the *Fbh1f* mRNA encodes an F-box-deleted protein when the second start codon is used. Also shown is the genomic structure of the *Fbh1f* (upper-right panel) and *Fbh1−* (lower-right panel) alleles. **B**. Establishment of homozygous *Fbh1f/f* and *Fbh1−/−* ES cell lines by gene targeting. Shown is genotype analysis of the WT, heterozygous, and homozygous mutant cell lines for each allele, using the primers depicted in A. **C**. The *Fbh1−* and *Fbh1f* alleles generate the predicted mRNA products. Shown are RT-PCR products from the WT, *Fbh1f/f*, and *Fbh1−/−* cell lines, using the primers depicted in the diagrams. **D**. The *Fbh1f* mRNA is efficiently translated. Shown are immunoblot signals for the Flag-epitope from transfections with empty vector (EV),

Fbh1-3xFlag (+), and Fbh1^f-3xFlag (f) expression plasmids in WT ES cells. (*) denotes a non-specific band from the Flag antibody.
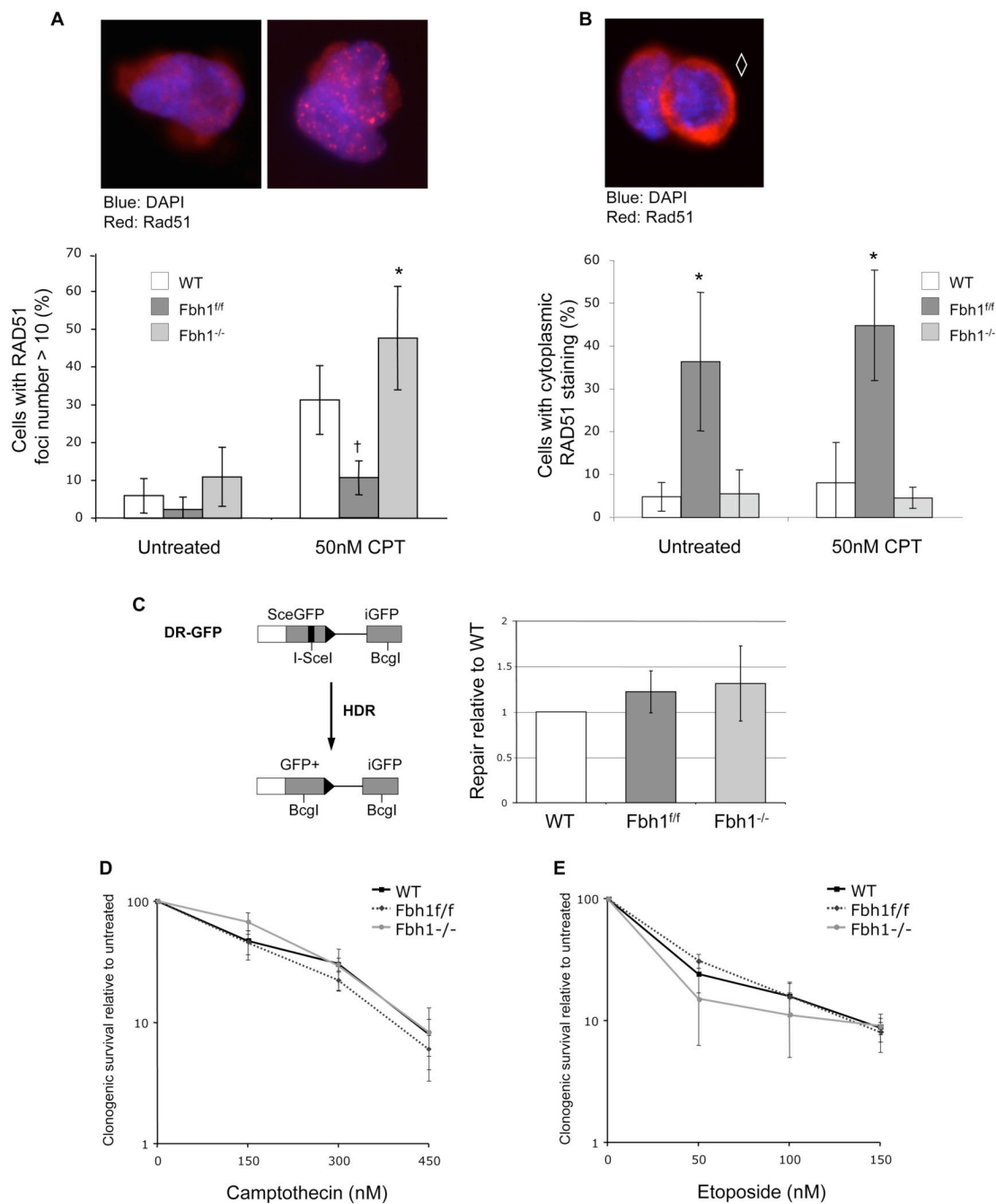
Blue: DAPI
Red: Rad51

Blue: DAPI
Red: Rad51

Fig. 2. Fbh1 deficiency affects Rad51 foci formation but not chromosome break repair
A. Top panel shows a representative image of WT cells without (left picture) or with (right picture) Rad51 foci after a 2-hour treatment with 50nM CPT. Bottom panel shows the percentage of cells with more than ten Rad51 foci for each sample. (*) denotes a statistical difference from WT (p=0.014). (†) denotes a statistical difference from WT (p<0.001). **B**. Top panel shows a representative image of *Fbh1^{f/f}* cells with cytoplasmic Rad51 immunostaining (◊). Bottom panel shows the percentage of cells with cytoplasmic Rad51 immunostaining without treatment or after 2 hours of 50nM CPT treatment. (*) denotes a statistical difference from WT (p<0.001). **C**. HDR is not affected by Fbh1-deficiency. The diagram shows the parental DR-GFP reporter, along with the HDR product of an I-SceI induced DSB, which

restores the *GFP* cassette. Shown is repair by HDR relative to WT. **D**. Camptothecin sensitivity is not affected by Fbh1-deficiency. Shown is the clonogenic survival of each cell line to the topoisomerase I poison, camptothecin. **E**. Etoposide sensitivity is not affected by Fbh1-deficiency. Shown is the clonogenic survival of each cell line to the topoisomerase II poison, etoposide.
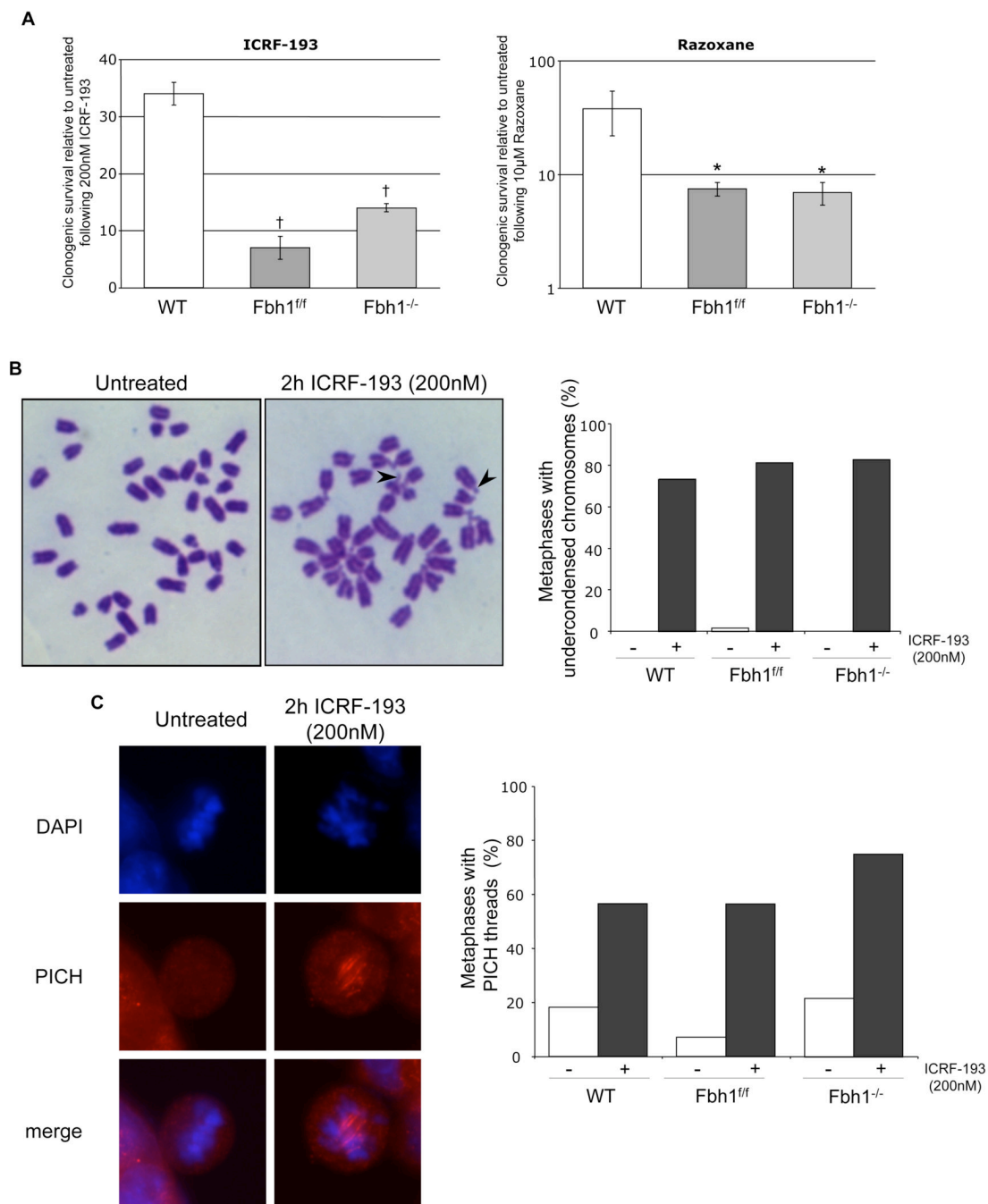
A

B

C

Fig. 3. Fbh1-deficient cells are sensitive to decatenation stress induced by ICRF-193 and razoxane
A. Clonogenic survival of each cell line to the bisdioxopiperazines ICRF-193 (left panel) and
razoxane (right panel). (†) denotes hypersensitivity compared to WT (p=0.0002), and (*)
denotes hypersensitivity compared to WT (p=0.03). **B**. Low-dose ICRF-193 treatment
primarily causes undercondensed centromeres. Left panel shows representative examples of
mitotic spreads from WT cells treated for 2 hours with ICRF-193 (200nM) or left untreated.
Arrows indicate two undercondensed centromeres. Right panel shows the percent of mitotic
spreads with evidence of at least three undercondensed chromosomes. For each sample, more
than 30 cells were analyzed. **C**. ICRF-193 treatment causes persistence of PICH threads in
mitosis. Left panel shows representative examples of mitotic cells with, or without, PICH

threads after a 2 hour treatment with ICRF-193 (200nM). Right panel shows the percentage of mitotic cells with PICH treads. For each sample, more than 30 cells were analyzed.
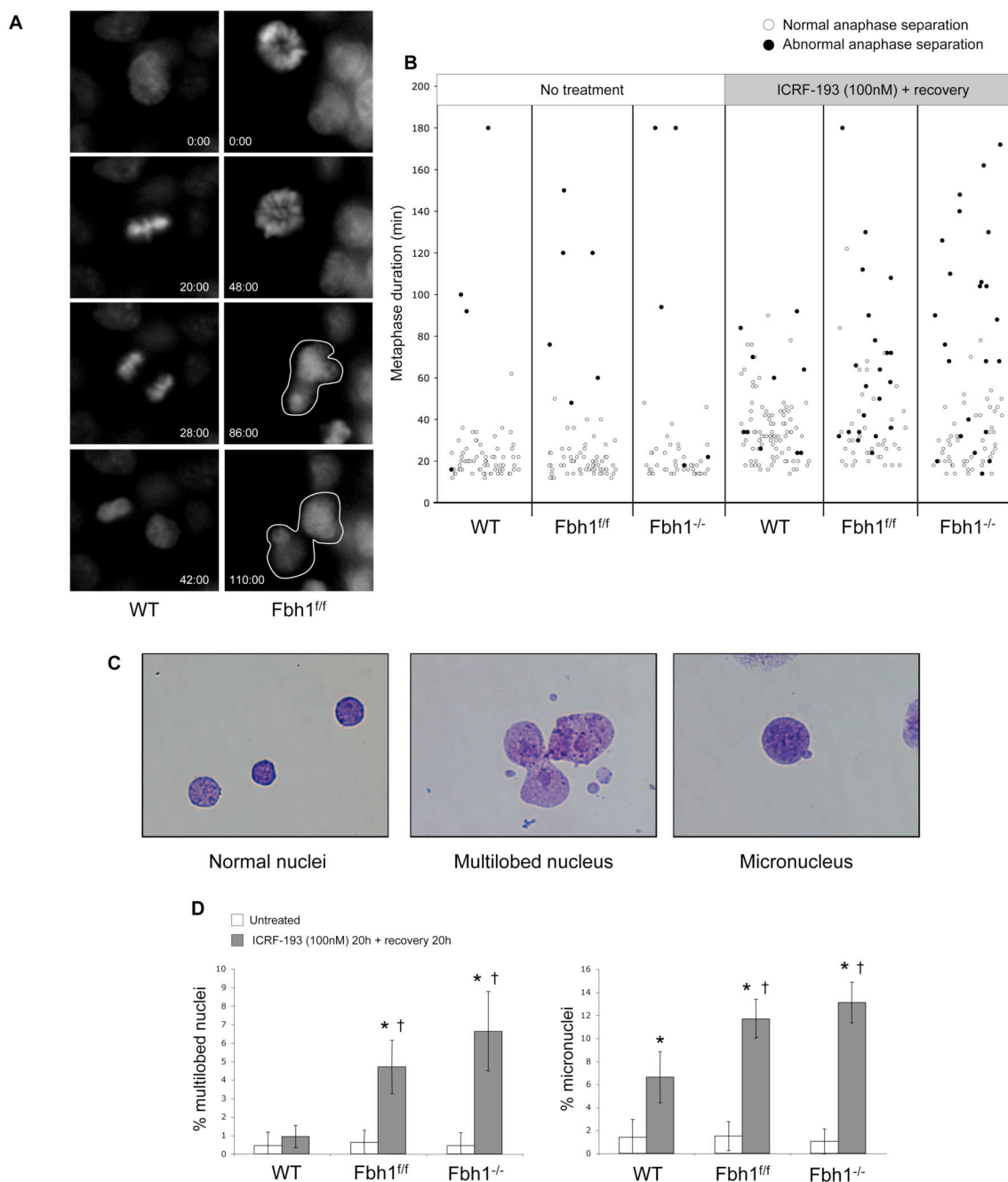
Fig. 4. Fbh1-deficient cells show defects in mitotic progression following decatenation stress
A. Real-time imaging of cells expressing H2B-GFP. Representative pictures of a normal
mitosis in WT cells (left panel) and of an abnormal mitosis in *Fbh1^{f/f}* cells after 20 hours
treatment with ICRF-193 (100nM) followed by 20 hours of recovery. Time of acquisition is
indicated in minutes. The white lines delineate aberrant nuclei resulting from abnormal
anaphase separation. **B**. Fbh1 is important to restore normal mitotic progression after
decatenation stress. WT and Fbh1-deficient cells were treated with ICRF-193 as in A, or left
untreated, and chromosome dynamics were analyzed by time-lapse microscopy as shown in
A. Shown for each cell line and treatment condition are individual cells scored for normal (○)
and abnormal (●) anaphase separation. The metaphase duration is represented by the placement

of each cell along the Y-axis. **C**. Representative images of normal nuclei, along with two classes of aberrant nuclei: micronuclei and multilobed nuclei. **D**. Fbh1-deficient cells show a marked elevation of aberrant nuclei following ICRF-193 treatment, compared to WT cells. Cells were treated with ICRF-193 as in A, or left untreated, and the morphology of individual nuclei was scored. Shown is the percentage of micronuclei and multilobed nuclei. (*) denotes a statistical difference from the untreated condition ($p < 0.001$). (†) denotes a statistical difference from WT cells ($p < 0.003$).

NIH-PA Author Manuscript

NIH-PA Author Manuscript

NIH-PA Author Manuscript

Table 1

	No treatment			ICRF-193 (100nM) + recovery		
	WT	**Fbh**$^{f/f}$	**Fbh1**$^{-/-}$	**WT**	**Fbh**$^{f/f}$	**Fbh1**$^{-/-}$
# mitotic cells with normal anaphase separation	67	61	43	88	41	52
# mitotic cells with abnormal anaphase separation	4	6	5	10	21	23
% mitotic cells with abnormal anaphase separation	5.6	9.0	14.3	10.2	33.9	30.7
P value (different from untreated)	-	-	-	*0.40*	*0.001*	*0.009*
P value (different from WT)	-	*0.52*	*0.48*	-	*0.004*	*0.001*